49th AIAA Aerospace Sciences Meeting including the New Horizons Forum and Aerospace Exposition
4 - 7 January 2011, Orlando, Florida

AIAA 2011-658

Check for updates

Conditional sampling and experiment design for quantifying manufacturing error of transonic airfoil

Han Chen*, Qiqi Wang†, Rui Hu‡
Massachusetts Institute of Technology, Cambridge, MA 02139, USA

Paul Constantine§
Sandia National Labs, Albuquerque, NM 87185, USA

Downloaded by STANFORD UNIVERSITY on August 20, 2018 | http://arc.aiaa.org | DOI: 10.2514/6.2011-658

We use conditional sampling of Gaussian stochastic processes to simulate the effect of manufacturing error on an RAE 2822 airfoil in transonic flow. Through a singular value decomposition of randomly sampled input-output Jacobian matrices, we show that the effect of the input high dimensional geometric uncertainty on the output aerodynamic performance can be largely attributed to a few dominant modes of the geometric perturbation. Based on this dimensionality reduction approach, we derive the "measurement information functions" of the dominant modes. We demonstrate that the measurement information function can be used to select a small number of inspection points on the airfoil surface, so that the uncertainty in the aerodynamic performance can be significantly reduced by measuring the manufacturing error on these points.

I. Introduction

Geometric variation in aerodynamic surfaces resulting from manufacturing errors has significant effect on their aerodynamic performance.[1,2] Due to the high cost of precise surface manufacturing techniques,[3] it is often impractical to remove the impact of these geometric variations by improving the manufacturing tolerance on wetted surfaces. Therefore, it is important to quantify the effect of manufacturing error on the performance of aerodynamic surfaces, as well as predicting the performance of individual surfaces with manufacturing error through measurements.

The relation between manufacturing errors on airfoils and their aerodynamic performance has previously been studied[4,5] In these work, the geometric variability due to manufacturing error is modeled with either principle component analysis, or Gaussian stochastic process models. The stochastic model of the manufacturing error is then sampled with Monte Carlo method. Computational fluid dynamics tools are used to predict the performance of each sample in order to quantify the effect of the manufacturing error. This knowledge can be used to improve the performance of airfoil blades under manufacturing uncertainties by modifying the baseline design so that it is less sensitive to manufacturing error.[6,7] Another type of optimization has been performed to find the optimal manufacturing tolerance for nacelles to minimize both the manufacturing cost and loss of aerodynamic performance.[8] Methods for inspecting aerodynamic surfaces with manufacturing error has also been extensively studied.[9–12]

In this paper, we use a conditional Gaussian stochastic process to model the manufacturing error on an airfoil surface. We present methods to perform Monte Carlo sampling of our conditional Gaussian process model, and use it to assess the effect of manufacturing error on the transonic performance of the

*Masters student, Aeronautics and Astronautics, Cambridge, MA, USA
†Corresponding author, Assistant Professor, Aeronautics and Astronautics, Cambridge, MA, USA, AIAA member
‡Postdoctoral scholar, Aeronautics and Astronautics, Cambridge, MA, USA, AIAA member
§John Von Neumann Research Fellow, Sandia National Laboratories, Albuquerque, NM, USA

Copyright © 2011 by the American Institute of Aeronautics and Astronautics, Inc. All rights reserved.

airfoil. The main contribution of this paper is a novel procedure for reducing the dimension of the high dimensional geometric variation based on the output aerodynamic quantities. The idea behind this dimension reduction technique is that the variation in the aerodynamic performance is largely determined by a small number of modes of the geometric variation. We find these dominant modes by performing a singular value decomposition of randomly sampled input-output Jacobian matrices. Based on the dimension reduction analysis, we present an approach to efficiently inspect airfoil surfaces with manufacturing error to reduce the uncertainties in its performance.

The paper is organized as following. Section II presents computational methods for sampling conditional Gaussian stochastic processes. Section III models the manufacturing error on an airfoil surface as conditional Gaussian processes, and analyzes the effect of the manufacturing error on the aerodynamic performance. Section IV presents our output-based input-space dimension reduction method, and its application on airfoil performance with manufacturing error. Section V addresses the question of how to inspect the airfoil surfaces in order to reduce the uncertainties in their aerodynamic performance. Section VI concludes this paper.

Downloaded by STANFORD UNIVERSITY on August 20, 2018 | http://arc.aiaa.org | DOI: 10.2514/6.2011-658

II. Conditional sampling of Gaussian processes

A. Sampling of Gaussian processes with Karhunen-Loeve expansion

A Gaussian random process $f(s,w), s \in [a,b], w \in \Omega$ is completely characterized by its mean function $\mu(s) = \mathbb{E}(f(s,w))$ and its covariance function $C(s_1,s_2) = \mathbb{E}(f(s_1,w)f(s_2,w)) - \mu(s_1)\mu(s_2)$. Such a process admits a Karhunen-Loeve expansion[13]

$$f(s,w) = \mu(s) + \sum_{k=1}^{\infty} \sqrt{\lambda_k}\, f_k(s)\, X_k(w), \tag{1}$$

where $X_k, k = 1,2,\ldots$ are independent standard Gaussian random variables; the deterministic functions f_k and the eigenvalues λ_k, $k = 1,2,\ldots$ are normalized solution of the eigenvalue problem

$$\int_a^b C(s_1,s_2)\, f_k(s_2)\, ds_2 = \lambda_k\, f_k(s_1), \quad \int_a^b f_k(s)^2\, ds = 1. \tag{2}$$

Because the covariance function C is positive-semi-definite, all λ_i are non-negative. They are ordered so that they are non-increasing, i.e., $\lambda_i \geq \lambda_{i-1}$ for all i.

This eigenvalue problem has known analytic solutions for certain stationary Gaussian processes.[14] When an analytic solution is not available, there are several methods for computing it numerically. When a small number of spatial grid points (several hundred) are sufficient to discretize the Gaussian process $f(s,w)$, the eigenvalue problem can be solved numerically by factorizing a symmetric, positive semi-definite matrix (the discrete covariance matrix). Alternatively, the eigen pairs of the most dominant modes can be calculated using a finite element approximation for f_k, which converts the infinite dimensional eigenvalue problem into a finite dimensional one. A third type of method, circulant embedding,[15] applies to quasi-stationary Gaussian processes whose covariance function takes the form of $C(s_1,s_2) = c(\|s_1 - s_2\|)$. This method approximates the Gaussian process by embedding it into a large enough periodic domain, where the eigenfunctions f_k are known to be sinusoidal functions. These eigenfunctions and the corresponding eigenvalues can be found by Fast Fourier Transform. This circular embedding approximation is particularly suitable for processes with small correlation length, i.e., the covariance function $c(\|s_1 - s_2\|)$ decays rapidly as $\|s_1 - s_2\|$ increases.

Once the eigen pairs $(f_k(s), \lambda_k)$ are computed, the Gaussian process can be sampled by truncating the Karhunen-Loeve expansion

$$f(s,w) \approx \mu(s) + \sum_{k=1}^{K} \sqrt{\lambda_k}\, f_k(s)\, X_k(w). \tag{3}$$

The order of truncation K is selected so that the truncated eigenvalues $\lambda_{K+1}, \lambda_{K+2}, \ldots$ are sufficiently small,

so that the truncated series retain most of the energy of the original random process, i.e.

$$\sum_{k=1}^{K} \lambda_k \approx \sum_{k=1}^{\infty} \lambda_k. \tag{4}$$

In the truncated Karhunen Loeve series (3), $X_1, X_2, \ldots, X_K$ are independent standard Gaussian random variables, and can be sampled using standard pseudo-random number generators.[16]

B. Conditional sampling of Gaussian processes with continuous method

A Gaussian process can be conditioned on a number of linear functionals of the process

$$\mathcal{G}_i(w) = \int_a^b g_i(s)\, f(s,w)\, ds\ , \quad i = 1, \ldots, L, \tag{5}$$

where each $g_i(s)$ is a deterministic generalized function. Some examples of the linear functional are

- Point measurement of f at a point s_0, when $g_i(s)$ is a Dirac delta $\delta(s - s_0)$.
- Linear combination of f at two points s_1 and s_2, when $g_i(s) = a_1\delta(s - s_1) + a_2\delta(s - s_2)$. The thickness of an airfoil is such an example, where s_1 and s_2 are corresponding points on the upper and lower surface.
- Derivative of f at a point,
- Second derivative of f at a point, such as curvature measurements.

We want to generate samples of a Gaussian process, given its mean and covariance functions, conditioned on given values of such linear functionals. Such conditional samples can be generated by either the continuous or discrete method. This subsection describes the continuous method.

The continuous method[17] calculates the modified mean and covariance functions of the conditional Gaussian process, then samples the conditional process using the same methods as sampling an unconditional Gaussian process. We denote the covariance matrix between $\mathcal{G}_i$ and $\mathcal{G}_j$ as D_{ij}, and the covariance between G_i the unconditional process $f(s)$ as $b_i(s)$. These quantities can be computed with

$$D_{ij} = Cov(\mathcal{G}_i, \mathcal{G}_j) = \int_a^b \int_a^b g_i(s_1)\, g_j(s_2)\, C(s_1, s_2)\ ds_1\, ds_2\ , \tag{6}$$

and

$$b_i(s) = Cov(f(s), \mathcal{G}_i) = \int_a^b g_i(s_1)\, C(s, s_1)\ ds_1\ , \tag{7}$$

Then the modified mean and covariance functions of the conditional process, conditioned on measurements $\mathcal{G}_i = d_i, i = 1, \ldots, L$, are given by[18]

$$\mu^c(s) = \mathbb{E}\left(f(s) \mid \mathcal{G}_i = d_i\right) = \mu(s) + \sum_{i,j=1}^{L} \left(D^{-1}\right)_{ij} b_i(s)\ (d_j - \mathbb{E}(\mathcal{G}_j)) \tag{8}$$

and

$$C^c(s_1, s_2) = Cov\left(f(s_1), f(s_2) \mid \mathcal{G}_i = d_i\right) = C(s_1, s_2) - \sum_{i,j=1}^{L} \left(D^{-1}\right)_{ij} b_i(s_1)\ b_j(s_2) \tag{9}$$

where $\left(D^{-1}\right)_{ij}$ is the i, j entry of the inverse of the covariance matrix D. These conditional mean and covariance functions completely describe the conditional process. Its Karhunen-Loeve expansion can be computed using methods described in Section A and used to produce conditional samples of Gaussian processes.

Downloaded by STANFORD UNIVERSITY on August 20, 2018 | http://arc.aiaa.org | DOI: 10.2514/6.2011-658

C. Discrete method for conditional sampling of Gaussian processes

Alternatively, conditional samples can be generated on the discrete level. In contrast to the continuous method, the Karhunen-Loeve expansion of the unconditional Gaussian process is first calculated and truncated; the conditional distribution of the expansion coefficients is then calculated and sampled accordingly.

This conditional distribution of the Karhunen-Loeve expansion coefficients is derived by plugging the Karhunen Loeve expansion into each linear functional of the Gaussian process, thus representing it as a linear combination of the coefficients, i.e.,

$$\begin{aligned}\mathcal{G}_i(w) &= \int_a^b g_i(s)\ f(s)\ ds \\ &= \int_a^b g_i(s)\ \mu(s)\ ds + \sum_{k=1}^{K} X_k(w)\ \sqrt{\lambda_k} \int_a^b g_i(s)\ f_k(s)\ ds \\ &= \mathbb{E}(\mathcal{G}_i) + \sum_{k=1}^{K} \alpha_{ik}\ X_k(w)\end{aligned} \tag{10}$$

where

$$\alpha_{ik} = \sqrt{\lambda_k} \int_a^b g_i(s)\ f_k(s)\ ds \tag{11}$$

Because $X_k, k = 1, \ldots, L$ are independent standard Gaussians, the covariance between $\mathcal{G}_i$ and a coefficient X_k is

$$Cov(\mathcal{G}_i, X_k) = \alpha_{ik}$$

Therefore, the conditional distribution of $X_k, k = 1, \ldots, L$ on $\mathcal{G}_i = d_i, i = 1, \ldots, L$ is a multi-variate Gaussian with mean

$$\mu_k^c = \mathbb{E}\left(X_k \mid \mathcal{G}_i = d_i\right) = \sum_{i,j=1}^{L} \left(D^{-1}\right)_{ij} \alpha_{jk} \left(d_i - \mathbb{E}(\mathcal{G}_i)\right) \tag{12}$$

and covariance matrix

$$C_{kl}^c = Cov\left(X_k, X_k \mid \mathcal{G}_i = d_i\right) = \delta_{kl} - \sum_{i,j=1}^{L} \left(D^{-1}\right)_{ij}\ \alpha_{ik}\ \alpha_{jl} \tag{13}$$

Note that δ_{kl} here is the Kronecker delta, not to be confused with Dirac delta in Section B. When the order of truncation K in Karhunen-Loeve expansion is small (no more than a few hundred), This multivariate Gaussian can be sampled by factorizing the covariance matrix. The resulting samples of X_k are then substituted into the truncated Karhunen-Loeve expansion of the unconditional process (3) to produce the desired conditional samples of the Gaussian process.

III. Estimating transonic performance of RAE 2822 airfoil with manufacturing errors

We model manufacturing error on an RAE 2822 airfoil as a Gaussian process perturbation in the surface normal direction. The Gaussian process is assumed to have zero mean, and a covariance function of

$$C(s_1, s_2) = \sigma^2\ \exp\left\{-\frac{(s_1 - s_2)^2}{2\,\lambda^2}\right\}$$

where s_1 and s_2 are positions along the airfoil, with $s = 0$ at the trailing edge, increases along the upper surface towards the leading edge and along the lower surface towards the trailing edge. In our analysis, all lengths are non-dimensionalized to the norminal chord length. For the RAE 2822 airfoil (shown in Figure 1), $0 \le s \le s_{\max} = 2.032$.

The following four models of the manufacturing error are analyzed:

Downloaded by STANFORD UNIVERSITY on August 20, 2018 | http://arc.aiaa.org | DOI: 10.2514/6.2011-658

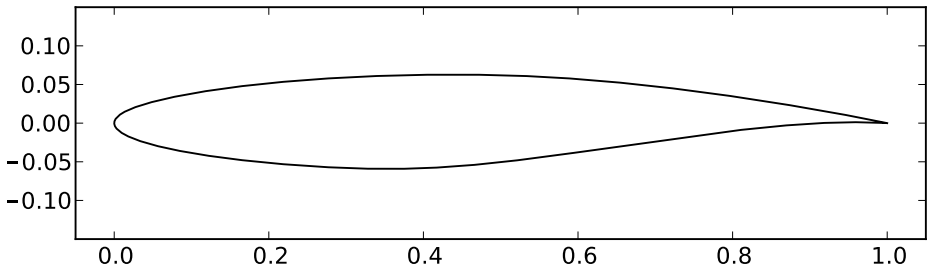

Figure 1. The norminal shape of the RAE 2822 airfoil

Downloaded by STANFORD UNIVERSITY on August 20, 2018 | http://arc.aiaa.org | DOI: 10.2514/6.2011-658

1. $\sigma = 0.0001$, $\lambda = 0.05$,
2. $\sigma = 0.0001$, $\lambda = 0.20$,
3. $\sigma = 0.0010$, $\lambda = 0.05$.
4. $\sigma = 0.0010$, $\lambda = 0.20$.

These cases covers precisely manufactured airfoils with manufacturing error of 0.01% of the chord length, and non-precisely manufactured airfoils with manufacturing error of 0.1% of the chord length. For each manufacturing precision, we analyze both the case when the manufacturing error is slowly varying, with a correlation length 20% of the chord length, and the case when the manufacturing error is more bumpy, with a correlation length 5% of the chord length.

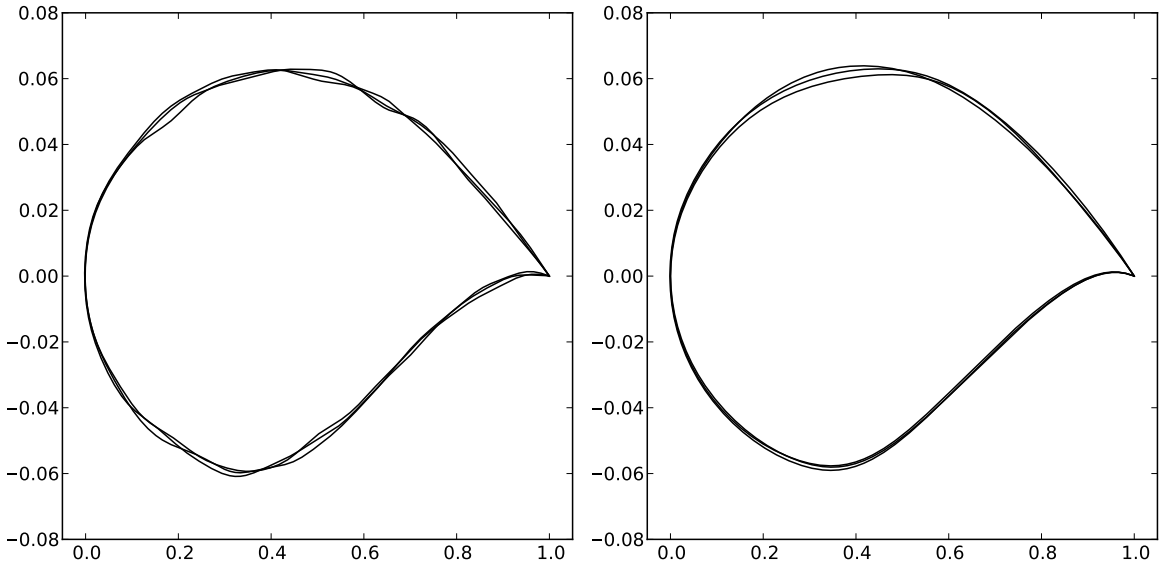

Figure 2. RAE 2822 airfoils with manufacturing errors of $\sigma = 0.001$, $\lambda = 0.05$ (left), and $\lambda = 0.20$ (right).

Figure 2 shows 3 samples of the non-precisely manufactured airfoils surface, with small and large correlation lengths, respectively. The y coordinate is magnified in order for the manufacturing to be visible. These samples are generated using method described in Section II, conditioned on the perturbation being 0 at the trailing edge, so that the airfoil surface is always closed.

The performance of the airfoils with randomly generated perturbations are simulated by solving the Euler equation. The freestream Mach number is 0.729, and the angle of attack for each airfoil sample is adjusted

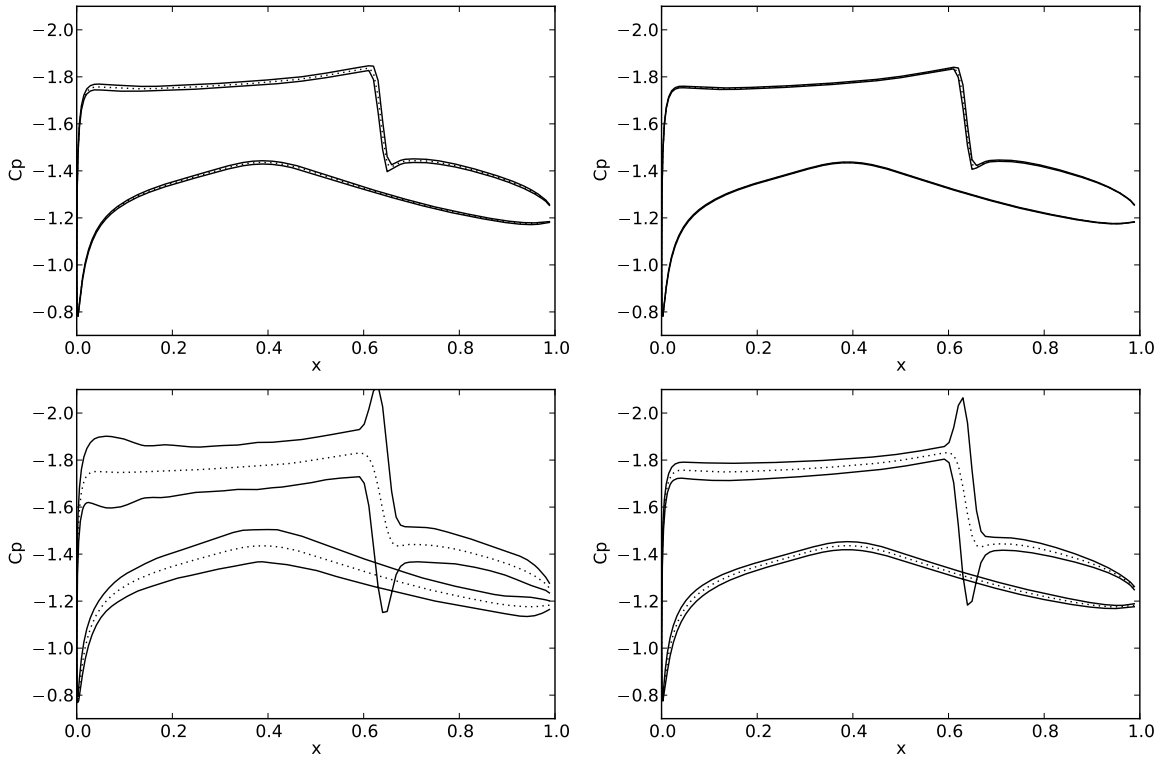

Figure 3. Surface pressure distribution of RAE 2822 airfoil with manufacturing error. Upper row: $\sigma = 0.0001$; lower row: $\sigma = 0.001$. Left column: $\lambda = 0.05$; right column: $\lambda = 0.20$.

so that a lift coefficient (non-dimensionalized with respect to the norminal chord length) of $c_l = 0.946$ is maintained. For the norminal airfoil shape, the corresponding angle of attack $\alpha = 2.31$ degrees. For each of the 4 manufacturing error models, 1024 samples are generated and simulated.

Figures 3 and 4 characterize the effect of the manufacturing error on the performance of the airfoil. Figure 3 shows the mean and 3-standard deviation interval of the surface pressure distribution. The effect on the Mach numbers is shown in Figure 4. The top plot shows the Mach number contour of the norminal geometry. The rest of the plots show contours of standard deviation of the Mach number caused by manufacturing errors: the first row corresponds to precisely manufactured airfoils ($\sigma = 0.0001$), and the second row corresponds to non-precisely manufactured airfoils ($\sigma = 0.001$). The manufacturing error affects the location and strength of the shock wave, resulting in a large standard deviation of pressure and Mach number around the shock wave. As expected, the pressure distribution of the precisely manufactured airfoils ($\sigma = 0.0001$) has less spread than the non-precisely manufactured airfoils ($\sigma = 0.001$). The smooth manufacturing error ($\lambda = 0.20$) has significantly less effect on surface pressure distribution than the more oscillatory manufacturing error ($\lambda = 0.05$) of the same magnitude, especially in areas away from the shockwave.

Figures 5 and 6 show the histograms of the aerodynamic coefficients c_m and c_d of the airfoils with manufacturing errors. Note that the lift coefficient c_l, instead of the angle of attack, is fixed in the simulations. The spread of these two output quantities of interest will be used as a baseline for our experiment design analysis described in Section V.

IV. Output based principle component analysis of Karhunen-Loeve modes

Given a set of airfoils manufactured with error, we can measure their shape and perform a flow simulation to find out the aerodynamic performance, i.e. c_d and c_m, of each specific airfoil. However, this is time

Downloaded by STANFORD UNIVERSITY on August 20, 2018 | http://arc.aiaa.org | DOI: 10.2514/6.2011-658

Downloaded by STANFORD UNIVERSITY on August 20, 2018 | http://arc.aiaa.org | DOI: 10.2514/6.2011-658

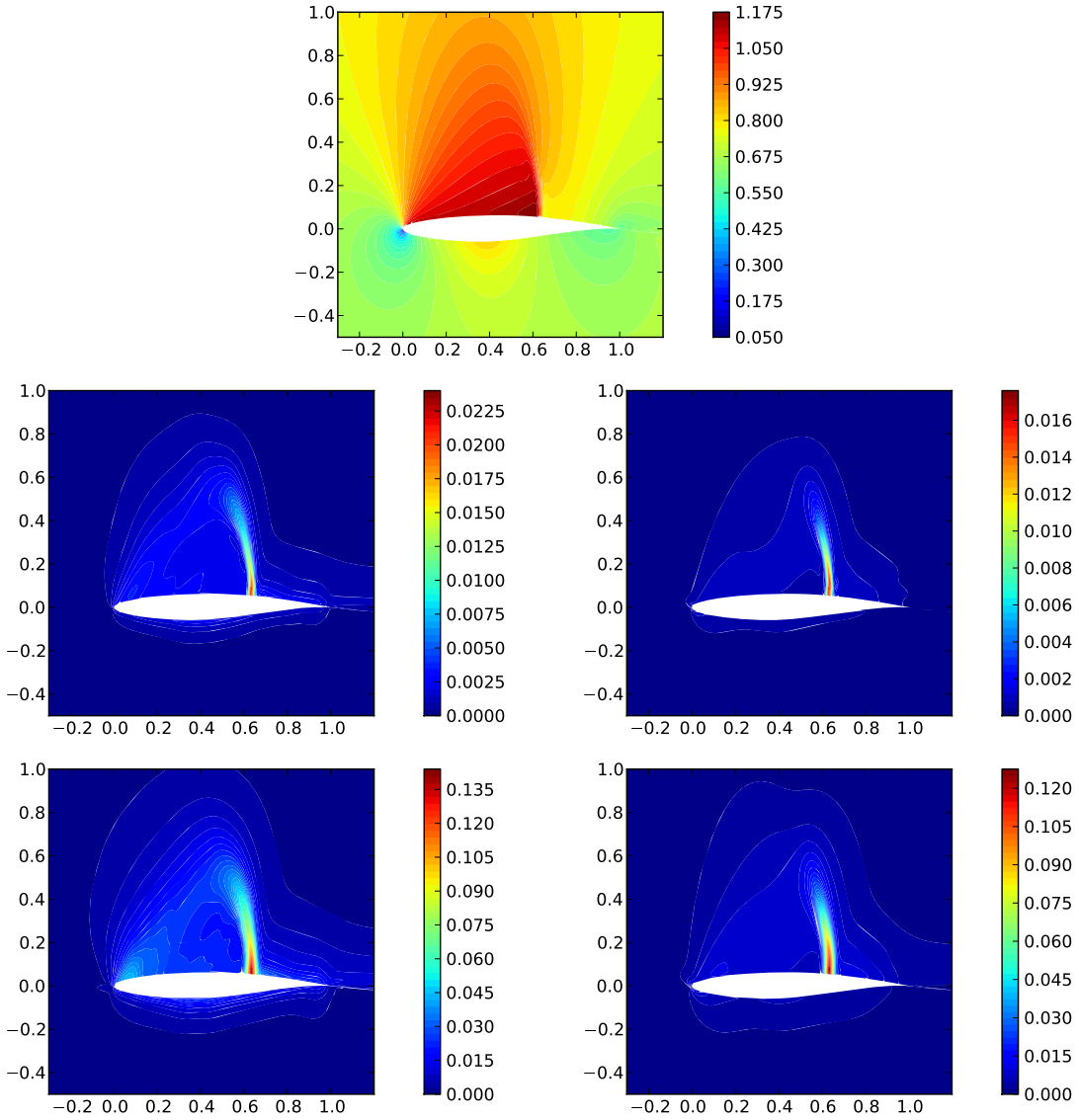

Figure 4. Mach number contour and Mach number standard deviation of RAE 2822 airfoil with manufacturing error.

consuming because the entire profile of each airfoil must be accurately measured. This section aims to overcome this difficulty by reducing the input space from a infinite dimensional, continuous representation of the manufacturing error, to a small number of linear combinations of the Karhunen Loeve modes.

Assuming that the truncated Karhunen-Loeve expansion (3) accurately represent the manufacture error, the aerodynamic performance of an airfoil can be expressed as

$$\vec{C} = \vec{C}(\vec{x}) \tag{14}$$

where where $\vec{C} = (c_d, c_m)^T$ and $\vec{x} = (x_1, \ldots, x_K)$ is a sample of the Karhunen-Loeve modes $X_1, \ldots, X_K$ in Equation (3), which are independent standard Gaussian random variables. This reduces the input parameter space from a infinite dimensional, continuous function, to a space of dimension K.

We then further reduce the dimension by a *global* sensitivity analysis. This global sensitivity analysis

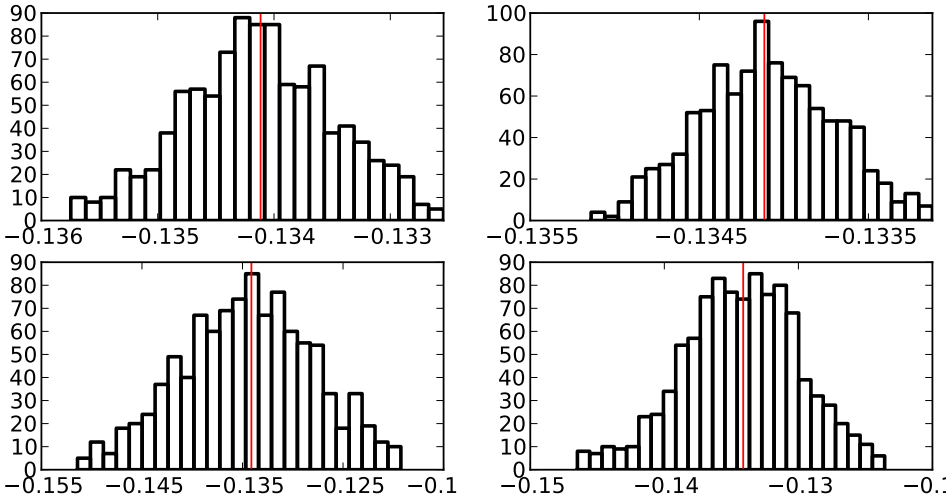

Figure 5. The c_m distribution of airfoils with manufacturing error.

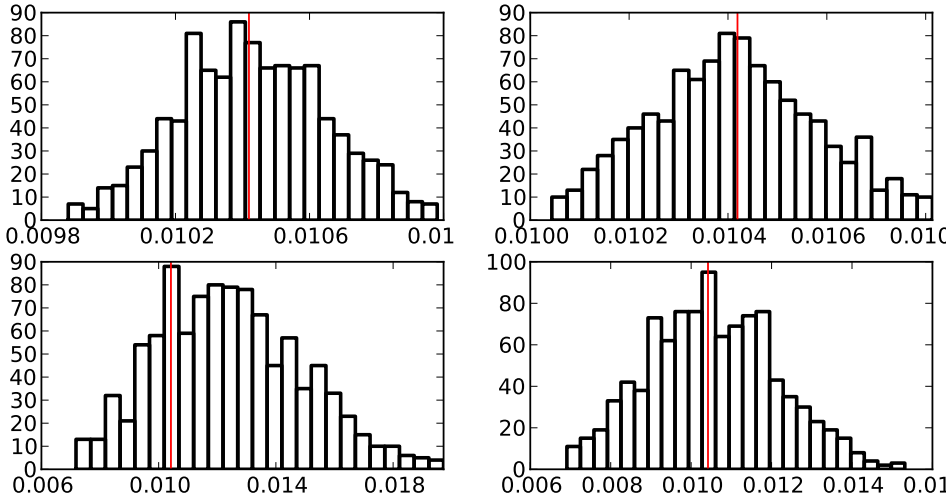

Figure 6. The c_d distribution of airfoils with manufacturing error.

finds out the *global nullspace* of $\vec{C}(\vec{x})$, i.e., the directions in the K-dimensional input space that the outputs are not sensitive to. Let

$$J(\vec{x}) = \frac{\partial \vec{C}}{\partial \vec{x}} \tag{15}$$

be the Jacobian matrix, which describes the *local* input-output sensitivity. We define the *global nullspace* as a linear space containing all vectors $\vec{u} = (u_1, \ldots, u_K)$ such that $\langle J(\vec{x}), \vec{u} \rangle = 0$ for all $\vec{x}$.

We find the global nullspace by computing the eigenvalues and eigenvectors of the matrix

$$\mathbb{E}\Big(J(\vec{X})^{\mathrm{T}} J(\vec{X})\Big) = U \Lambda U^{\mathrm{T}}, \tag{16}$$

where the expectation is taken on $\vec{X} = (X_1, \ldots, X_K)$. Suppose Λ contains L nonzero eigenvalues, and the rest of the K eigenvalues are (almost) zero. The nullspace of this matrix, spanned by the $K - L$ eigenvectors in U corresponding to the zero eigenvalues, is the global nullspace of $\vec{C}(\vec{x})$. This is because if $\vec{u}$ is in the

Downloaded by STANFORD UNIVERSITY on August 20, 2018 | http://arc.aiaa.org | DOI: 10.2514/6.2011-658

nullspace, then

$$0 \;=\; \vec{u}^{\,\mathrm{T}}\,\mathbb{E}\Big(J^{\mathrm{T}}J\Big)\,\vec{u} \;=\; \mathbb{E}\Big(\|J\,\vec{u}\,\|_2^2\Big) \tag{17}$$

Therefore, $J(\vec{x})\,\vec{u} = 0$ almost surely for any $\vec{x}$.

The singular value decomposition (16) can be used to reduce the dimension of the input space. Define the transformed Karhunen-Loeve modes $Y_1, \ldots, Y_K$ as

$$\begin{pmatrix} Y_1 \\ Y_2 \\ \vdots \\ Y_K \end{pmatrix} = U^{\mathrm{T}} \begin{pmatrix} X_1 \\ X_2 \\ \vdots \\ X_K \end{pmatrix} \tag{18}$$

Let $\vec{y} = (y_1, \ldots, y_K)$ be a sample of $Y_1, \ldots, Y_K$ corresponding to $\vec{x} = (x_1, \ldots, x_K)$, then $\vec{y} = U^{\mathrm{T}}\vec{x}$, $\vec{x} = U\,\vec{y}$, and

$$\frac{\partial \vec{C}}{\partial y_k} = \frac{\partial \vec{C}}{\partial \vec{x}}\frac{\partial \vec{x}}{\partial y_k} = J(\vec{x})\,u_k \tag{19}$$

where u_k is the kth column of the matrix U, i.e., the kth eigenvector of $\mathbb{E}\Big(J^{\mathrm{T}}J\Big)$. For $k > L$, u_k is in the global nullspace, thus

$$\frac{\partial \vec{C}}{\partial y_k} = J(\vec{x})\,u_k = 0 \tag{20}$$

almost everywhere for $k = L+1, \ldots, K$. As a result, the outputs can be determined from the transformed Karhunen-Loeve modes with reduced dimensionality:

$$\vec{C} = \vec{C}(y_1, \ldots, y_L) \tag{21}$$

We implement the idea above by the following procedure:

1. Generate $N = 1024$ samples of conditional Gaussian process (fixed in the trailing edge), and generate the corresponding perturbed airfoil shape.
2. Solve each airfoil, compute the drag coefficient c_d and c_m at $c_l = 0.946$ by solving the Euler equation.
3. For each sample, we evaluate the local Jacobian $J(\vec{x})$ with respect to the first 20 Karhunen-Loeve modes ($K = 20$) by performing linear regression with its 50 nearest samples.
4. We compute the singular value decomposition of the stacked Jacobian matrix

$$\frac{1}{\sqrt{N}} \begin{pmatrix} J(\vec{x}_1) \\ \vdots \\ J(\vec{x}_N) \end{pmatrix} = V\,\sqrt{\Lambda}\,U^{\mathrm{T}} \tag{22}$$

where $\vec{x}_i$ are randomly sampled Karhunen-Loeve coefficients. Then the eigenvalue decomposition (16) can be approximated with

$$\mathbb{E}\Big(J^{\mathrm{T}}J\Big) \approx \frac{1}{N}\sum_{i=1}^{N} J(\vec{x}_i)^{\mathrm{T}}J(\vec{x}_i) = \Big(J(\vec{x}_1)^{\mathrm{T}} \ldots J(\vec{x}_N)^{\mathrm{T}}\Big) \begin{pmatrix} J(\vec{x}_1) \\ \vdots \\ J(\vec{x}_N) \end{pmatrix} = U\,\Lambda\,U^{\mathrm{T}} \tag{23}$$

This approach avoids the expensive evaluation of the Monte Carlo covariance matrix itself, and is more numerically stable because the stacked Jacobian matrix has only square root of the condition number of the matrix $\mathbb{E}\Big(J^{\mathrm{T}}J\Big)$.

Downloaded by STANFORD UNIVERSITY on August 20, 2018 | http://arc.aiaa.org | DOI: 10.2514/6.2011-658

The resulting matrix U determines the transform between the Karhunen-Loeve modes $X_k, k = 1, \ldots, K$ and the transformed Karhunen-Loeve modes $Y_k, k = 1, \ldots, K$ through Equation (18). The entries of the diagonal matrix Λ determines which of the transformed modes have significant effect on the output aerodynamic coefficients.

This procedure is applied to the aerodynamic performance of RAE 2822 airfoils with manufacturing errors. We perform an analysis with the output being $\vec{C} = c_m$, an analysis with $\vec{C} = c_d$, and an joint analysis with $\vec{C} = (c_m, c_d)$. Figure 7 shows the normalized singular values for the joint analysis and separate analysis for the $\lambda = 0.05$, $\sigma = 0.0010$ case. These normalized singular values are the entries of the diagonal matrix Λ in Equation (22), scaled so that the largest value equal to 1.

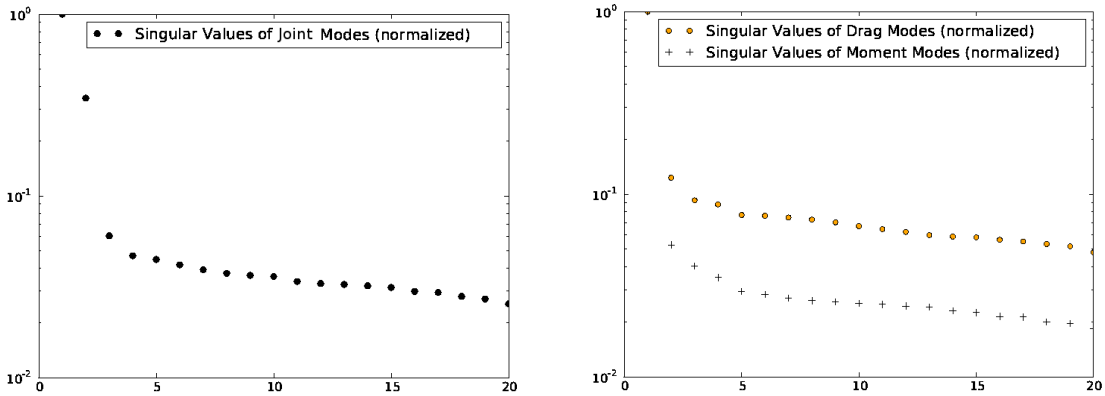

Figure 7. Scaled singular values of the joint analysis (left) and of the separate analysis (right).

In the joint analysis, only two modes Y_1 and Y_2 are dominant, thus the 20 dimensional parameter space can be effectively reduced to 2. In the analysis with output $\vec{C} = c_m$, only one mode $Y_1^{c_m}$ is dominant; and only one mode $Y_1^{c_d}$ is dominant in the analysis with output being c_m.

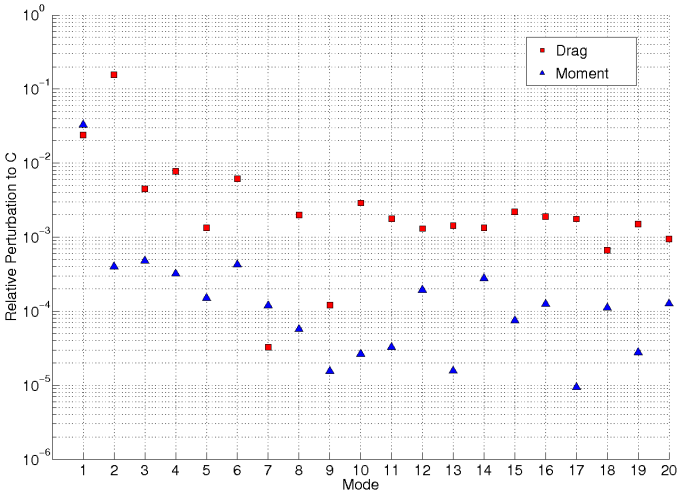

Figure 8. Sensitivity of c_d and c_m to the transformed Karhunen-Loeve modes Y_k.

We further analyze the result of the joint analysis by evaluating the sensitivity of c_d and c_m to the two dominant modes Y_1 and Y_2. The result is shown in Figure 8. Both c_d and c_m are sensitive to the first mode

Downloaded by STANFORD UNIVERSITY on August 20, 2018 | http://arc.aiaa.org | DOI: 10.2514/6.2011-658

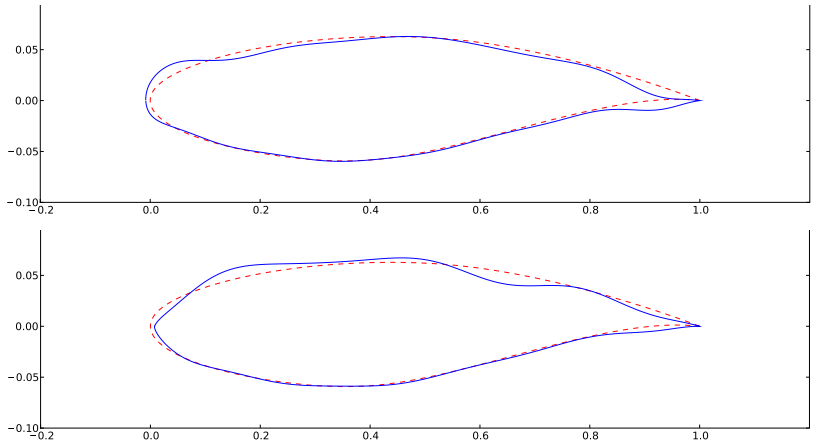

Figure 9. Y_1 **(upper) and** Y_2 **(lower) perturbed airfoil. The dashed line is the norminal airfoil.**

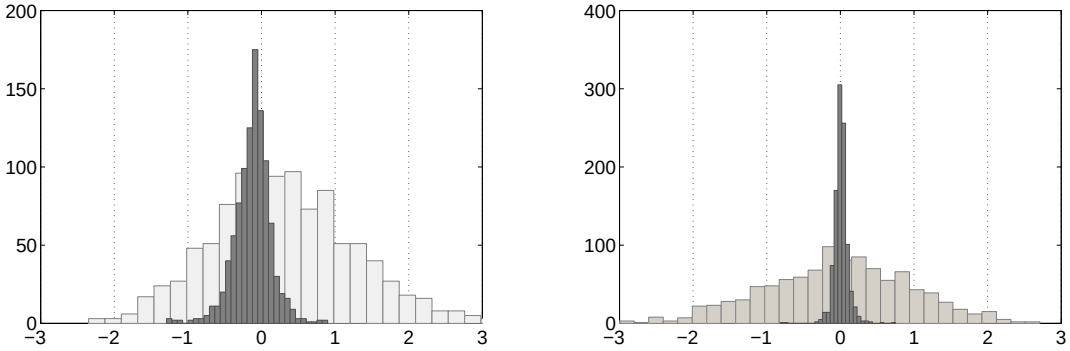

Figure 10. The dark histogram shows the deviation between $\tilde{C}$ **and** C **(dark histogram) compared against the deviation of** C **with the norminal value. Left plot:** $C = c_d$**; right plot:** $C = c_m$**. The x-axes are normalized by the standard deviations of** C**.**

Y_1, while only c_d is sensitive to the second mode Y_2. The airfoil perturbed by Y_1 and Y_2 is shown in Figure 9, the coefficient of each mode is set to a very large value for visualization purpose. We can see that Y_1 has large perturbations at the trailing and leading edges in opposite directions, which explains why c_m is very sensitive to this mode; Y_2 has large bumps at both ends of the supersonic region, causing c_d to be sensitive to this mode.

To demonstrate the effectiveness of the dimensionality reduction approach, we use a simple bivariate quadratic polynomial to approximate $\vec{C}(Y_1, Y_2) = (c_m(Y_1, Y_2), c_d(Y_2, Y_2))$ with our 1024 samples. We denote the resulting polynomial approximation as $\tilde{C}(Y_1, Y_2) = (\tilde{c}_m(Y_1, Y_2), \tilde{c}_d(Y_2, Y_2))$. The approximation error $\tilde{C} - \vec{C}$ is compared against the spread of $\vec{C}$ in Figure 10. This result indicates that we can effectively reduce the infinite dimensional functional $\vec{C}$ that depends on a continuous surface, to a two dimensional function $\vec{C}(Y_1, Y_2)$. With a simple two-dimensional surrogate function, we can largely determine the values of $\vec{C}$ from the two transformed Karhunen-Loeve modes Y_1 and Y_2.

Downloaded by STANFORD UNIVERSITY on August 20, 2018 | http://arc.aiaa.org | DOI: 10.2514/6.2011-658

V. Designing airfoil inspection points via measurement information function

Let

$$\begin{pmatrix} Y_1^{c_d} \\ Y_2^{c_d} \\ \vdots \\ Y_K^{c_d} \end{pmatrix} = U^{c_d} \begin{pmatrix} X_1 \\ X_2 \\ \vdots \\ X_K \end{pmatrix}, \quad \begin{pmatrix} Y_1^{c_m} \\ Y_2^{c_m} \\ \vdots \\ Y_K^{c_m} \end{pmatrix} = U^{c_m} \begin{pmatrix} X_1 \\ X_2 \\ \vdots \\ X_K \end{pmatrix} \tag{24}$$

be the transformed Karhunen-Loeve modes for c_d and c_m, respectively. $Y_1^{c_d}$ is the mode that c_d is most sensitive to, and $Y_1^{c_m}$ is the mode that c_m is most sensitive to.

Assume an airfoil with manufacturing error is measured at inspection points $s_1, s_2, \ldots, s_m$. The measurements are sufficiently accurate compared to the manufacturing error, so that the measurement error can be ignored. With these measurements, the magnitude of the manufacturing error at these inspection points $f(s_1), \ldots, f(x_m)$ is known. In this section, we want to choose these inspection points, so that the uncertainty in the airfoil performance given these measurements is small, i.e., we want to minimize the conditional variance

$$\min_{s_1,\ldots,s_m} Var\Big(c_d \mid f(s_i), \ldots, f(s_m)\Big) \qquad \min_{s_1,\ldots,s_m} Var\Big(c_m \mid f(s_i), \ldots, f(s_m)\Big) \tag{25}$$

Because of the nonlinear aerodynamic relation between the shape of the airfoil and its performance, Equation (25) is a nonlinear optimal experimental design problem, and can be difficult to solve. Therefore, instead of directly minimizing the conditional variance of c_d and c_m, we seek to minimize the conditional variance of the transformed Karhunen-Loeve modes that c_d and c_m are most sensitive to, i.e., we minimize the conditional variance

$$\min_{s_1,\ldots,s_m} Var\Big(Y_1^{c_d} \mid f(s_i), \ldots, f(s_m)\Big) \qquad \min_{s_1,\ldots,s_m} Var\Big(Y_1^{c_m} \mid f(s_i), \ldots, f(s_m)\Big) \tag{26}$$

Without loss of generality, we solve the first part of Problem (26) by analyzing the covariance structure of both $Y_k^{c_d}, k = 1, \ldots, K$ and $f(s_i), i = 1, \ldots, m$.

$$Cov \begin{pmatrix} Y_1^{c_d} \\ \vdots \\ Y_K^{c_d} \\ f(s_1) \\ \vdots \\ f(s_m) \end{pmatrix} = \begin{pmatrix} I & A \\ A^{\mathrm{T}} & B \end{pmatrix}. \tag{27}$$

I is the $K \times K$ identity matrix, because $Y_k^{c_d}, k = 1, \ldots, K$ are independent standard Gaussian random variables. The $M \times M$ matrix B contains the covariance of the inspection points, i.e.

$$B_{ij} = Cov(f(s_i), f(s_j)) = \sigma^2 \ \exp\left\{\frac{(s_i - s_j)^2}{2\,\lambda^2}\right\} \tag{28}$$

The matrix A contains the covariance between the transformed Karhunen-Loeve modes

$$Y_i^{c_d} = \sum_{k=1}^{K} U_{ik}^{c_d} X_k$$

and the measurements

$$f(s_j) = \sum_{k=1}^{K} \sqrt{\lambda_k}\ f_k(s_j)\ X_k$$

Downloaded by STANFORD UNIVERSITY on August 20, 2018 | http://arc.aiaa.org | DOI: 10.2514/6.2011-658

Because the (untransformed) Karhunen-Loeve modes X_k are independent standard Gaussians, $\mathbb{E}(X_i\, X_j) = \delta_{ij}$. Also, both $Y_i^{c_d}$ and $f(s_j)$ has zero mean; therefore,

$$A_{ij} = Cov\left(Y_i^{c_d}, f(s_j)\right) = \mathbb{E}\left(Y_i^{c_d} f(s_j)\right) = \sum_{k=1}^{K} U_{ik}^{c_d} \sqrt{\lambda_k}\; f_k(s_j) \tag{29}$$

The conditional covariance of $Y_k^{c_d}, k = 1, \ldots, K$ given $f(s_i), i = 1, \ldots, m$ can be computed from the joint covariance matrix (27):

$$Cov\left(\begin{array}{c|c} Y_1^{c_d} & f(s_1) \\ \vdots & \vdots \\ Y_K^{c_d} & f(s_m) \end{array}\right) = I - A\, B^{-1} A^{\mathrm{T}} \tag{30}$$

In particular, the variance of the first transformed Karhunen-Loeve mode $Y_1^{c_d}$ is the top-left entry of the conditional covariance matrix,

$$Var\left(Y_1^{c_d} \;\middle|\; f(s_1), \ldots, f(s_m)\right) = 1 - A_1\, B^{-1} A_1^{\mathrm{T}}\,, \tag{31}$$

where A_1 is the first row of the matrix A.

In order to gain insight in how to choose the measurement point $s_1, \ldots, s_m$ to make the conditional variance (31) small, we make a further simplification. This simplification is made based on the assumption that the spacing between the inspection points $s_1, \ldots, s_m$ are large compared to the correlation length λ of the random process describing the manufacturing error. Under this assumption, the covariance between the inspection points reduces to

$$Cov(f(s_i), f(s_j)) \approx \sigma^2\, \delta_{ij}\,,$$

and thus the covariance function of the measurements reduces to

$$B \approx \sigma^2\, I$$

Plug this into Equation (31), we get

$$Var\left(Y_1^{c_d} \;\middle|\; f(s_1), \ldots, f(s_m)\right) \approx 1 - \frac{1}{\sigma^2}\, A_1\, A_1^{\mathrm{T}} \tag{32}$$

Define the **measurement information function**

$$a^{c_d}(s) = \frac{1}{\sigma} \sum_{k=1}^{K} U_{1k}^{c_d} \sqrt{\lambda_k}\; f_k(s) \tag{33}$$

Then

$$Var\left(Y_1^{c_d} \;\middle|\; f(s_1), \ldots, f(s_m)\right) \approx 1 - \sum_{i=1}^{m} \left(a^{c_d}(s_i)\right)^2 \tag{34}$$

This simplified formula (34) for the conditional variance gives two very simple criteria for choosing the measurement location in order to make the conditional variance small:

- We want to choose s_i where the measurement information function $a^{c_d}(s)$ has large magnitude.
- We want to choose s_i to be far away from each other (compared to the correlation length of the measurement error), so that the assumption made to diagonalize B is valid.

In the rest of this section, we compute the measurement information functions $a^{c_d}(s)$ and $a^{c_m}(s)$ for the RAE 2822 airfoil with measurement errors, select inspection points based on these two criteria, and analyze the transonic performance of the airfoil conditioned on the measurements.

Downloaded by STANFORD UNIVERSITY on August 20, 2018 | http://arc.aiaa.org | DOI: 10.2514/6.2011-658

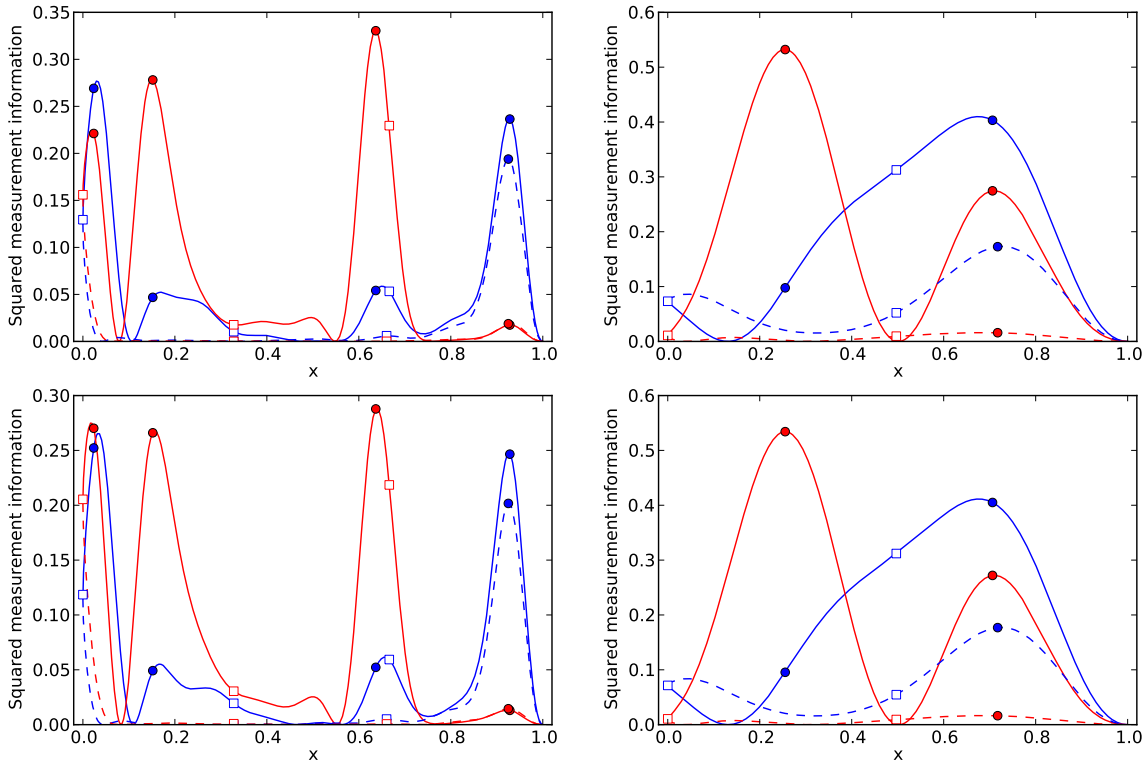

Figure 11. The squared measurement information functions $(a^{c_m}(s))^2$ (blue) and $(a^{c_d}(s))^2$ (red), on upper (solid lines) and lower (dashed lines) sides of the airfoil surface. Left column: $\lambda = 0.05$; right column: $\lambda = 0.20$; upper row: $\sigma = 0.0001$; lower row: $\sigma = 0.001$.

Figure 12. The location of the designed inspection points and uniformly spaced inspection points on the airfoil. Left: $\lambda = 0.05$; right: $\lambda = 0.20$.

Figure 11 shows the squared measurement information functions for both the transformed Karhunen-Loeve coefficient that c_m is most sensitive to $((a^{c_m}(s))^2$, shown as blue lines), and the transformed Karhunen-Loeve coefficient that c_d is most sensitive to $((a^{c_d}(s))^2$, shown as red lines). The solid lines plot the squared measurement information functions on the upper surface of the airfoil, and the dashed lines correspond to the lower surface.

We choose a set of inspection points according to our criteria. These **designed inspection points** are plotted as filled circles in Figure 12. For the $\lambda = 0.05$ cases, 5 inspection points are selected, 4 on the upper surface and one on the lower surface. The value of the measurement information at these points are marked with blue and red filled circles in the left plots in Figure 11, for c_m and c_d, respectively. For the $\lambda = 0.2$ case, 3 inspection points are selected, 2 on the upper surface and 1 on the lower surface. The value of the measurement information function at these points are marked in the right plots in Figure 11. These inspection points are designed so that either $(a^{c_m}(s))^2$ or $(a^{c_d}(s))^2$ has large magnitude at these points. They are also sufficiently far away from each other compared to the correlation length of the manufacturing error.

Downloaded by STANFORD UNIVERSITY on August 20, 2018 | http://arc.aiaa.org | DOI: 10.2514/6.2011-658

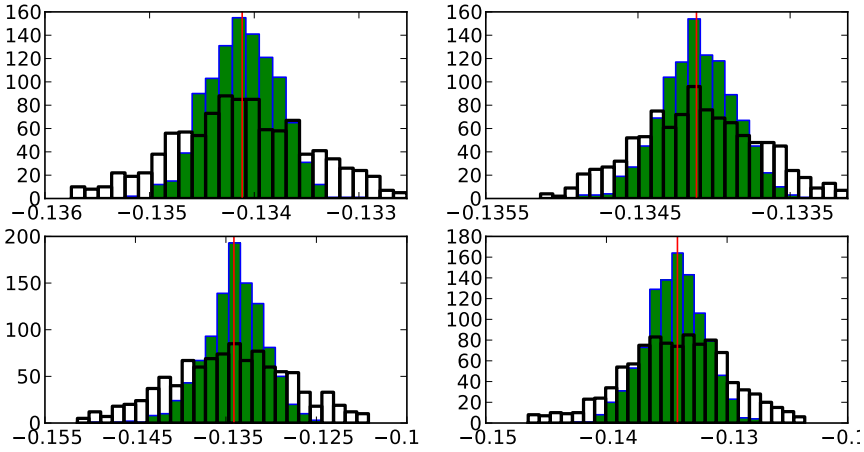

Figure 13. The distribution of c_m of airfoils with manufacturing error conditioned on measurements on *designed* inspection points. Left column: $\lambda = 0.05$; right column: $\lambda = 0.20$; upper row: $\sigma = 0.0001$; lower row: $\sigma = 0.001$.

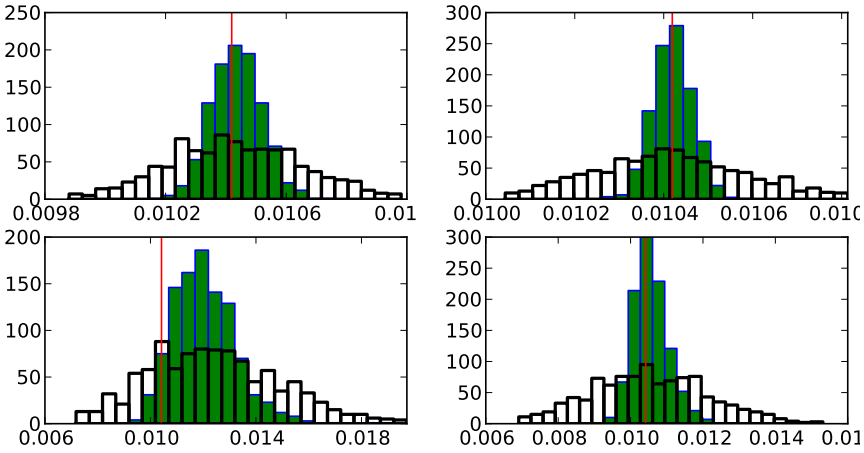

Figure 14. The distribution of c_d of airfoils with manufacturing error conditioned on measurements on *designed* inspection points. Left column: $\lambda = 0.05$; right column: $\lambda = 0.20$; upper row: $\sigma = 0.0001$; lower row: $\sigma = 0.001$.

The spread in aerodynamic performance of airfoils conditioned on measurements at these designed inspection points is shown in Figures 13 and 14. In this study, 1024 samples of the RAE 2822 airfoils with manufacturing error are generated, conditioned on that the manufacturing error at the designed inspection points (shown as filled circles in Figure 12) is equal to 0. The flow field for each airfoil is computed by solving the Euler equation, and the resulting histogram aerodynamic coefficients is shown as green bars in Figures 13 and 14. The white bars are the distribution of aerodynamic coefficients of airfoils without conditioning on any measurements, as also shown in Figures 5 and 6. This comparison between the conditioned aerodynamic coefficients and the unconditioned aerodynamic coefficients shows that *knowing the manufacturing error at the designed measurements points significantly reduces the uncertainty in the aerodynamic performance of the airfoil.*

For comparison, we perform a similar analysis with *uniformly spaced* inspection points, instead of the *designed* inspection points based on the measurement information functions. The same number of inspection points are used (5 for the $\lambda = 0.05$ cases, and 3 for the $\lambda = 0.20$ cases). The location of the uniformly spaced inspection points are shown as open squares in Figure 12. The value of the squared measurement information functions are also plotted as open squares in Figure 11. The histogram of aerodynamic coefficients c_m and

Downloaded by STANFORD UNIVERSITY on August 20, 2018 | http://arc.aiaa.org | DOI: 10.2514/6.2011-658

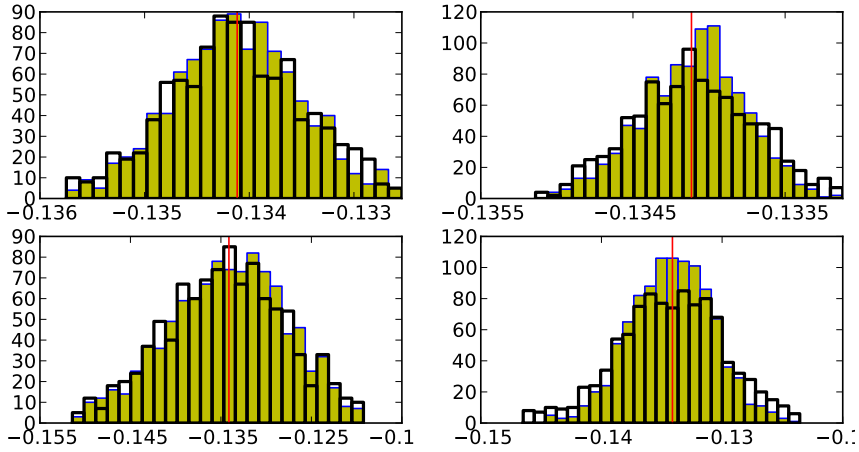

Figure 15. The distribution of c_m of airfoils with manufacturing error conditioned on measurements on *uniform* points. Left column: $\lambda = 0.05$; right column: $\lambda = 0.20$; upper row: $\sigma = 0.0001$; lower row: $\sigma = 0.001$.

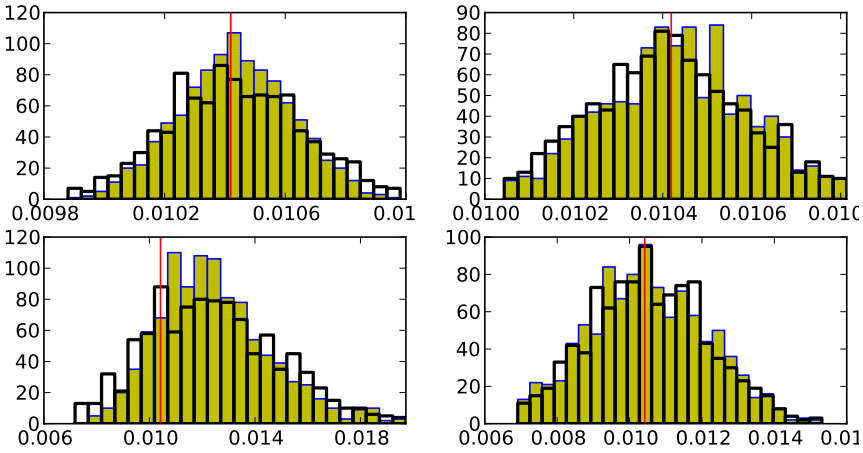

Figure 16. The distribution of c_d of airfoils with manufacturing error conditioned on measurements on *uniform* points. Left column: $\lambda = 0.05$; right column: $\lambda = 0.20$; upper row: $\sigma = 0.0001$; lower row: $\sigma = 0.001$.

c_d conditioned on the manufacturing error being 0 at these uniformly spaced inspection points are shown as yellow bars in Figures 15 and 16. The white histogram is the unconditioned case, for comparison purpose. These figures demonstrate that knowing the manufacturing error at *uniformly spaced* points reveals much less information on the aerodynamic performance than knowing the manufacturing error at the *designed* inspection points. This is explained by the fact that the measurement information function does not have large magnitude at the uniformly spaced points, as shown in Figure 11.

VI. Conclusion

We demonstrate a method of quantifying the effect of manufacturing error in transonic flow simulations. The manufacturing error on an aerodynamic surface is modeled as a Gaussian random processes with geometric constraints. Methods for discretization and Monte Carlo sampling of these conditional Gaussian processes are discussed. We present results on how the correlation structure of the random process affects the pressure distribution and aerodynamic coefficients of a RAE 2822 airfoil in transonic flow.

With the Karhunen-Loeve expansion of the Gaussian process model, the aerodynamic performance of

Downloaded by STANFORD UNIVERSITY on August 20, 2018 | http://arc.aiaa.org | DOI: 10.2514/6.2011-658

the airfoil as a functional of the continuous geometric variation can be reduced to a finite dimensional function of the truncated Karhunen-Loeve modes. We demonstrate that the dimension of these function can be further reduced using a global sensitivity analysis. Through singular value decomposition of randomly sampled Jacobian matrices, we find the global nullspace of the Karuhnen-Loeve modes, and compute the small number of dominant transformed Karhunen-Loeve modes that largely determines the output quantities.

In order to assess the aerodynamic performance of a particular airfoil manufactured with error, we only need to know the values of the dominant transformed Karhunen-Loeve modes. However, they cannot be measured directly. We derived the measurement information functions, which reveals the amount of information in the dominant modes that can be gained from inspecting the manufacturing error at a point on the airfoil. We demonstrate that the uncertainty in the aerodynamic performance can be significantly reduced by measuring the manufacturing error at a small number of points where the measurement information functions have large magnitude; while measuring the manufacturing error at such small number of uniformly spaced points has almost no effect in reducing the uncertainty.

Downloaded by STANFORD UNIVERSITY on August 20, 2018 | http://arc.aiaa.org | DOI: 10.2514/6.2011-658

References

[1]Roberts., W. B., "Axial compressor performance restoration by blade profile control," *AIAA-84-GT-232, ASME*, 1984.

[2]Bailey, M. W., "First order manufacturing constraints and requirements," *Integrated Multidisiplinary Design of High Performance Multistage Compressor Systems*, 1998, p. 3.13.27.

[3]Curran, R., Kundu, A., Raghunathan, S., and McFadden, R., "First order manufacturing constraints and requirements," *Proceedings of the Institution of Mechanical Engineers, Part G: Journal of Aerospace Engineering*, Vol. 216, No. 1, 2002.

[4]Lamb, C. T. and Darmofal, D. L., "Performance-Based Geometric Tolerancing of Compressor Blades," *ASME Conference Proceedings*, Vol. 2004, No. 41707, 2004, pp. 203–210.

[5]Garzon, V. E. and Darmofal, D. L., "Impact of Geometric Variability on Axial Compressor Performance," *Journal of Turbomachinery*, Vol. 125, No. 4, 2003, pp. 692–703.

[6]Lamb, C. M., *Probabilistic Performance-Based Geometric Tolerancing of Compressor Blades*, Master's thesis, Massachusetts Institute of Technology, 2003.

[7]Kumar, A., Keane, A., Nair, P., and Shahpar, S., "Robust design of compressor blades against manufacturing variations," *Proceedings of the 2006 ASME International Design Engineering Technical Conferences & Computers and Information In Engineering Conference*, 2006.

[8]K., K. A., J., W., S., R., and R., M., "Parametric optimization of manufacturing tolerances at the aircraft surface," *Journal of Aircraft*, Vol. 39, No. 2, 2002.

[9]Badar, M. A., Raman, S., and Pulat, P. S., "Experimental verification of manufacturing error pattern and its utilization in form tolerance sampling," *International Journal of Machine Tools and Manufacture*, Vol. 45, No. 1, 2005, pp. 63 – 73.

[10]Obeidat, S. and Raman, S., "An intelligent sampling method for inspecting free-form surfaces," *International Journal of Advanced Manufacturing Technology*, Vol. 40, No. 11-12, 2009, pp. 1125–1136.

[11]Badar, M., Raman, S., Pulat, P., and Shehab, R., "Experimental analysis of search-based selection of sample points for straightness and flatness estimation," *Journal of Manufacturing Science and Engineering, Transactions of the ASME*, Vol. 127, No. 1, 2005, pp. 96–103.

[12]Li, Y. and Gu, P., "Free-form surface inspection techniques state of the art review," *Computer-Aided Design*, Vol. 36, No. 13, 2004, pp. 1395 – 1417.

[13]Loeve, M., *Probability Theory, Vol. II*, Springer-Verlag, New York, 1978.

[14]Ghanem, R. and Spanos, P. D., *Stochastic Finite Elements: A Spectral Approach*, Dover Publications, New York, 2003.

[15]Dietrich, C. R. and Newsam, G. N., "Fast and exact simulation of stationary Gaussian processes through circulant embedding of the covariance matrix," *SIAM J. Sci. Comput.*, Vol. 18, No. 4, 1997.

[16]Devroye, L., *Non-Uniform Random Variate Generation*, Springer-Verlag, New York, 1986.

[17]Davis, M. W., "Production of conditional simulations via the LU triangular decomposition of the covariance matrix," *Mathematical Geology*, Vol. 19, 1987.

[18]Stein, M. L., *Interpolation of Spatial Data: Some Theory for Kriging*, Springer, New York, 1999.